



Irasema Alcántara-Ayala
Željko Arbanas
David Huntley
Kazuo Konagai
Snježana Mihalić Arbanas
Matjaž Mikoš

Maneesha V. Ramesh
Kyoji Sassa
Shinji Sassa
Huiming Tang
Binod Tiwari
Editors

Progress in Landslide Research and Technology Volume 2 Issue 2, 2023



OPEN ACCESS

Progress in Landslide Research and Technology

The Open Access book series of the International Consortium on Landslides (ICL) aims to be the common platform for the publication of recent progress in landslide research and technology for practical applications and the benefit of society contributing to the Kyoto Landslide Commitment 2020, which is expected to continue up to 2030 and even beyond for the global promotion of understanding and reducing landslide disaster risk as well as the 2030 Agenda Sustainable Development Goals. The contributions include original and review articles, case studies, activity reports and teaching tools for the promotion of understanding and reducing landslide disaster risks.

Irasema Alcántara-Ayala • Željko Arbanas •
David Huntley • Kazuo Konagai •
Snježana Mihalić Arbanas • Matjaž Mikoš •
Maneesha V. Ramesh • Kyoji Sassa •
Shinji Sassa • Huiming Tang • Binod Tiwari
Editors

Progress in Landslide
Research and Technology,
Volume 2 Issue 2, 2023

Contents

Part I ICL Landslide Lesson

- Advancements in Shear Strength Interpretation, Testing, and Use for Landslide Analysis** 3
Binod Tiwari and Beena Ajmera
- Rock Avalanches in the Tibetan Plateau of China** 55
Yufeng Wang, Qiangong Cheng, Qiwen Lin, Anwen Shi, Jie Ming, Zhiyi Feng, and Zhang Song

Part II Original Articles

- Landslide Susceptibility Zonation Using GIS-Based Frequency Ratio Approach in the Kulon Progo Mountains Area, Indonesia** 115
Egy Erzagian, Wahyu Wilopo, and Teuku Faisal Fathani
- Physically-Based Regional Landslide Forecasting Modelling: Model Set-up and Validation** 127
Veronica Tofani, Elena Benedetta Masi, and Guglielmo Rossi
- Consequence: Frequency Matrix as a Tool to Assess Landslides Risk** 137
Michel Jaboyedoff
- Do not Let Your Guard Down: Landslide Exposure and Local Awareness in Mexico** 155
Ricardo J. Garnica-Peña and Irasema Alcántara-Ayala
- Landslides in Higher Education Curricula and Beyond** 167
Matjaž Mikoš
- Community Scale Landslide Resilience: A Citizen-Science Approach** 183
Maneesha Vinodini Ramesh, Hemalatha Thirugnanam, Nitin Kumar Mohanan, Balmukund Singh, Harichandana C Ekkirala, and Ramesh Guntha
- Remedial Measures Impact on Slope Stability and Landslide Occurrence in Small-Scale Slope Physical Model in 1 g Conditions** 197
Željko Arbanas, Josip Peranić, Vedran Jagodnik, Martina Vivoda Prodan, and Nina Čeh
- Surficial Geology and Geomorphology of the North Slide, Thompson River Valley, British Columbia, Canada: Application of Fundamental Geoscience Information to Interpretations of Geospatial Monitoring Results** 221
David Huntley, Drew Rotheram-Clarke, Kelvin Sattler, and David Elwood

High Resolution Numerical Weather Simulation for Orographic Precipitation as an Accurate Early Warning Tool for Landslide Vulnerable Terrains	239
H. A. A. I. S. Bandara and Ryo Onishi	
Climate Change as Modifier of Landslide Susceptibility: Case Study in Davao Oriental, Philippines	247
Mary Antonette A. Beroya-Eitner, May Celine T. M. Vicente, Julie Mae B. Dado, Marion Roel S. Dimain, Joel T. Maquiling, and Faye Abigail T. Cruz	
Fractal-Based Evaluation of the Spatial Relationship Between Conditioning Factors and the Distribution of Landslides (a Case Study in Tinh Tuc, Cao Bang Province, Vietnam)	259
Binh Van Duong, Igor K. Fomenko, and Kien Trung Nguyen	
Procedure of Data Processing for the Improvement of Failure Time Prediction of a Landslide Based on the Velocity and Acceleration of the Displacement	269
Imaya Ariyaratna and Katsuo Sasahara	
Numerical Analysis of the Effect of Rainfall on the Stability of Sandstone-Covered Mudstone Cutting Slopes	285
Ying Guo, Yating Du, Wei Shan, and Chengcheng Zhang	
Part III Review Articles	
Post-formation Behavior of Hattian Landslide Dam and Post-breaching Situation	299
Ahsan Sattar and Kazuo Konagai	
Investigation of Debris Flow Impact Mechanisms and Designs	311
Charles W. W. Ng, Sunil Poudyal, Haiming Liu, Aastha Bhatta, W. A. Roanga K. De Silva, and Zhenyang Jia	
A Review of the Disaster Risk Assessment Perspectives	323
Dayan Munasinghe, Terrance Fernando, Kaushal Keraminiyage, and Asiri Karunawardena	
Part IV IPL Projects, World Centres of Excellence on Landslide Risk Reduction, and Kyoto Landslide Commitment 2020	
Application of LAND-SUITE for Landslide Susceptibility Modelling Using Different Mapping Units: A Case Study in Croatia	343
Sanja Bernat Gazibara, Marko Sinčić, Mauro Rossi, Paola Reichenbach, Martin Krkač, Hrvoje Lukačić, Petra Jagodnik, Gabrijela Šarić, and Snježana Mihalić Arbanas	
An Integrated Approach to Landslides Risk Management for Local and National Authorities	355
Biljana Abolmasov, Miloš Marjanović, Uroš Đurić, and Jelka Krušić	
Assessing Landslide Hazard in the High City of Antananarivo, Madagascar (UNESCO Tentative Site)	361
William Frodella, Daniele Spizzichino, Giacomo Lazzeri, Claudio Margottini, Veronica Tofani, and Nicola Casagli	

Part V ICL Landslide Teaching Tools

Teaching Tool for LS-Tsunami	375
Khang Dang, Kyoji Sassa, and Doan Huy Loi	

Part VI Technical Notes and Case Studies

ClirtheRoads: An Integrated Approach to Landslide Risk Management on Roads in Serbia	403
Biljana Abolmasov, Ranka Stanković, Miloš Marjanović, Nikola Vulović, and Uroš Đurić	

Part VII World Landslide Reports

Rock Slope Instabilities Affecting the AIUla Archaeological Sites (KSA)	413
José Ignacio Gallego, Claudio Margottini, Ingrid Perissé Valero, Daniele Spizzichino, Tommaso Beni, Daniela Boldini, Francesca Bonometti, Nicola Casagli, Riccardo Castellanza, Giovanni Battista Crosta, Paolo Frattini, William Frodella, Giovanni Gigli, Edoardo Lusini, Serena Rigamonti, Giulia Rusconi, and Lorenzo Vitrano	
Refugees' Perception of Landslide Disasters: Insights from the Rohingya Camps in Cox's Bazar, Bangladesh	431
A. S. M. Maksud Kamal, Anika Samm-A, Bayes Ahmed, and Peter Sammonds	
KLC2020 Official Promoters	441
Geological Survey of Canada, Natural Resources Canada	443
Faculty of Civil and Geodetic Engineering, University of Ljubljana	447
China University of Geosciences, Wuhan	451
Department of Civil Engineering, National Taiwan University	457
Institute of Cold Regions Science and Engineering, Northeast Forestry University	461
Marui & Co. Ltd.	463
Nippon Koei Co., Ltd., Geohazard Management Division	467
Ellegi Srl	471
Chuo Kaihatsu Corporation	475
Godai Kaihatsu Corporation	479
Kiso-Jiban Consultants Co. Ltd	483
Kokusai Kogyo Co. Ltd	485
OSASI Technos, Inc.	489
List of ICL Members	493
Index	497



Fractal-Based Evaluation of the Spatial Relationship Between Conditioning Factors and the Distribution of Landslides (a Case Study in Tinh Tuc, Cao Bang Province, Vietnam)

Binh Van Duong, Igor K. Fomenko, and Kien Trung Nguyen

Abstract

This paper presents the assessment results of the spatial relationship between past landslides and four landslide factors in Tinh Tuc town, Cao Bang province, Vietnam, including distance to roads, distance to faults, distance to drainage, and distance to geological boundaries. The fractal dimension values were determined using fractal analyses on three sets of raw data, including the number of landslides, landslide density, and landslide relative density. Using a combination of the frequency ratio (FR) method and the fractal method, landslide susceptibility maps were produced to determine which raw data set more properly analyzes the role of factors in the development of the landslide process. Assessment results using the receiver operating characteristic (ROC) method indicate that the fractal analysis of the raw data sets successfully determines the spatial relationship between conditioning factors and landslides in the study area. In addition, relationship analyses using datasets based on landslide density provide more optimal outcomes. The authors also suggest integrating the fractal method with other quantitative assessment methods to improve the accuracy of landslide prediction in Vietnam and worldwide.

Keywords

Fractal method · Landslide · Conditioning factor · Spatial relationship · Frequency ratio method · Tinh Tuc · Vietnam

1 Introduction

The challenge of ensuring the sustainable development of residential communities in the context of rapid urbanization is crucial for developing countries, including Vietnam. With 75% of the territory comprised of mountainous terrain, the frequency of sediment-related natural hazards has increased in recent years (Lan Huong et al. 2022). Consequently, it is necessary to identify hazard zones by producing integrated maps based on the current situation and available materials. These maps include data on the spatial distribution of hazard zones and their temporal evolution. These data are essential for evaluating potential risks, long-term territorial planning, and land use planning.

Compared to other sediment-related disasters, landslides are prevalent in Vietnam, particularly in the northern mountainous regions, and negatively impact the sustainable development of local communities (Thanh Thi Pham et al. 2020). Therefore, numerous studies on landslides have been conducted in these regions (Bien et al. 2022; Hung et al. 2017). According to previous studies, most landslides were triggered by precipitation, and the increase in landslide frequency has been associated with human activities (e.g., road construction) (Do et al. 2022; Tien Bui et al. 2017). When developing models for predicting landslides, determining the relationship between conditioning factors and the distribution of landslides is crucial (Liao et al. 2022). The evaluation results may validate the correctness of the selection of analysis factors and play a significant role in the performance of the prediction models.

This paper presents the results of the fractal-based evaluation of the spatial relationship between conditioning factors

B. Van Duong (✉)

Department of Engineering Geology, Ordzhonikidze Russian State Geological Prospecting University, Moscow, Russia

Department of Engineering Geology, Hanoi University of Mining and Geology, Hanoi, Vietnam

e-mail: duongvanbinh@humg.edu.vn

I. K. Fomenko

Department of Engineering Geology, Ordzhonikidze Russian State Geological Prospecting University, Moscow, Russia

K. T. Nguyen

Department of Hydrogeology and Engineering Geology, Institute of Geological Sciences, Vietnam Academy of Science and Technology, Hanoi, Vietnam

and the distribution of landslides in Tinh Tuc town, Cao Bang province, Vietnam. The spatial relationship was evaluated using three raw data sets, including the number of landslides, relative landslide density, and landslide density. By producing landslide susceptibility zonation maps, this study determined that all three data sets are suitable for assessing the relationship between landslide occurrences and conditioning factors. In addition, this study determined that the prediction model based on relative landslide density and landslide density provided a higher performance in analyzing the relationship between landslides and conditioning factors.

2 Study Area

Cao Bang province (6690 km²; 22° 21' N to 23° 07' N and 105° 16' E to 106° 50' E), which is located in the northeastern mountainous region of Vietnam (Fig. 1), has experienced numerous natural disasters in recent years, especially landslides, due to the influence of various natural, environmental, and social conditions. Nguyen Binh is a mountainous district in the southern portion of Cao Bang province that is

determined to be one of the areas with a very high likelihood of landslides (VIGMR 2017).

Tinh Tuc town is 18 km from the center of Nguyen Binh district and is situated on National Highway 34, which connects Cao Bang province and Ha Giang province (Fig. 1). The study area covers a total of 66.76 km², including Tinh Tuc town and its surroundings. The elevation of the study area ranges from 434 m in the valley to 1876 m in the mountainous terrain, where Phia Oac peak reaches 1932 m (Kien et al. 2021). The studied territory is characterized by geological formations and complexes composed of igneous and sedimentary rocks dated from the Paleozoic to the Quaternary period. The weathering process has contributed to the growth of two main types of weathering crust in the study area: ferosialite (86%) and sialferite (14%). In 2020, a failure volume of 2500 m³ was recorded at Highway 34, Km 192 + 500, on the 3–4 m-thick weathering crust formed from the rocks of the Song Hien formation (Fig. 2a). Another landslide occurred in 2016 at Km 200 + 300 on Highway 34. The weathering crust, with a thickness between 3 and 4 m, formed from the Cao Bang Complex rocks, has produced a sliding mass with a volume of 50,000 m³ (Fig. 2b).

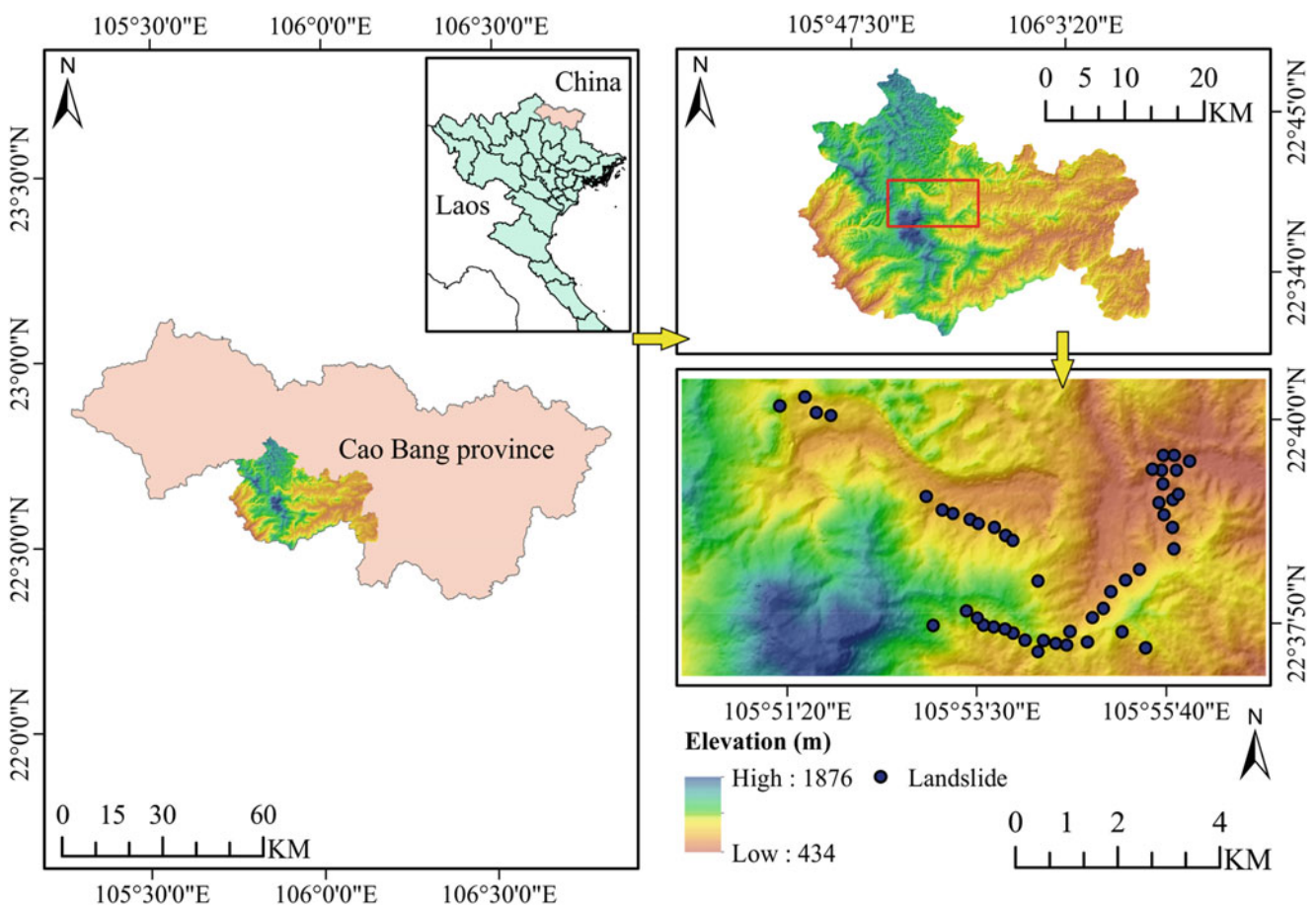


Fig. 1 Location of study area



Fig. 2 Landslides at the national highway 34 km 192 + 500 (a), and at Km 200 + 300 (b). Photo by T. K. Nguyen

Heavy rainfall in a short period of time or prolonged rainfall events have been identified as the trigger of landslides in the study area.

3 Evaluation of the Spatial Relationship Between Conditioning Factors and the Distribution of Landslides

3.1 Methods

Mandelbrot (1967), who initially introduced the fractal theory in his study of the British coastline, determined that the degree of complication of a geographic curve may be characterized by a “dimension” D . Since then, the fractal method has been improved and extensively utilized in numerous fields of research, including medicine (Tanabe et al. 2020), muscle activity patterns during locomotion (Santuz and Akay 2020), materials science (Paun et al. 2022), the characterization of absorption capacity, porosity, and surface area (Elejalde-Cadena and Moreno 2021), natural hazards (Cello and Malamud 2006), etc.

In the landslide susceptibility study, the fractal method is employed to determine the weights of the conditioning factors, therefore indicating the role of each conditioning factor in the occurrence of landslides in the studied territory. The method may be characterized as a power law described by Eq. (1):

$$p(r) \propto C \cdot r^{-D} \quad (1)$$

where r is the feature measured scale, p is the measured value under the corresponding scale r , C is a constant value, and D is the fractal dimension (Hu et al. 2020). Fractal analyses provide a raw data set (P) based on several variables, such as the number of landslides, relative landslide density, and

landslide density. The cumulative sum (S) values are then determined using the formula (2):

$$\{P\} = \{P_1, P_2, \dots, P_n\}$$

$$\{S_1\} = \{P_1, P_1 + P_2, \dots, P_1 + P_2 + \dots + P_n\}$$

$$\{S_2\} = \{S_{11}, S_{11} + S_{12}, \dots, S_{11} + \dots + S_{1n}\} \dots \dots \dots (2)$$

The fractal analysis then constructs the (S , r) graphs and performs a linear fitting to determine the D value for each condition factor. By using the formula (3), the weight of each landslide conditioning factor (W_i) is calculated:

$$W_i = D_i / \sum_{i=1}^n D_i \quad (3)$$

In this study, the Frequency ratio (FR) was integrated with the Fractal method to produce partition landslide susceptibility zonation (LSZ) maps to examine the efficacy of spatial relationship evaluation using different raw data sets. The FR method evaluates the relationship between the distribution of landslides and the subclasses of conditioning factors (Wang et al. 2020) based on the formula (4):

$$FR_i = \%LS_i / \%A_i \quad (4)$$

where FR_i is the FR value of subclass i , $\%LS_i$ is the percentage of landslides in subclass i , and $\%A_i$ is the area percentage of subclass i . The calculated FR value is then normalized to the weight of the factor class (NFR) according to the formula (5):

$$NFR_i = FR_i / \sum_{i=1}^n FR_i \quad (5)$$

Finally, the landslide susceptibility index (LSI) is calculated according to the formula (6):

$$LSI = \sum_{i=1}^n NFR_i \times W_i \tag{6}$$

3.2 Spatial Relationship Between Conditioning Factors and Landslide Distribution

For analyzing the spatial relationship, this study selected four landslide conditioning factors, including distance to roads, distance to faults, distance to drainage, and distance to geological boundaries. Downloaded OpenStreetMap data from Geofabrik was used to produce a map of the distance to roads in the study area (Fig. 3a). Along with a 12.5-m-resolution digital elevation model (DEM), data on geological

units and fault systems were provided by the Institute of Geological Sciences, Vietnam Academy of Science and Technology. Geologically, the study area has six geological units, including the Bac Son formation, Dong Dang formation, Song Hien formation, Quaternary deposits, Cao Bang complex, and Pia Oac complex. Afterward, these data were used to prepare additional factor maps, including distance to faults (Fig. 3b), distance to drainage (Fig. 3c), and distance to geological boundaries (Fig. 3d). Each factor was divided into subclasses for quantifying the relationship between conditioning factors and landslide distribution. Distance to roads, distance to faults, and distance to geological boundaries were subdivided into 11 subclasses, while the distance to drainage was subdivided into seven classes, as shown in Table 1.

Analysis of the spatial relationship between conditioning factors and past landslides revealed that most landslides occurred within 100 m of roads and 200 m of drainage systems. This result demonstrates that the construction of

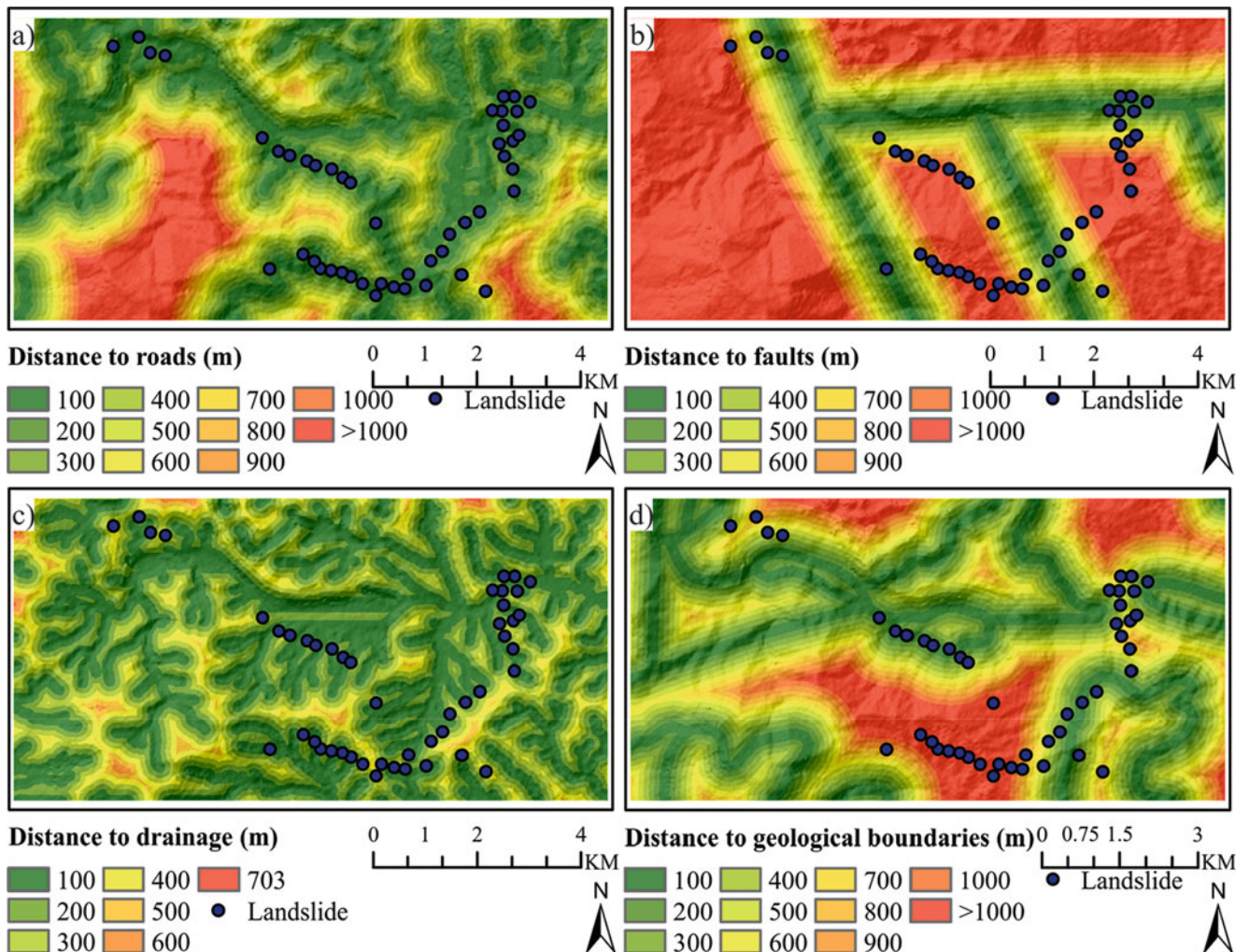


Fig. 3 Maps of distance to roads (a), distance to faults (b), distance to drainage (c), and distance to geological boundaries (d)

Table 1 Spatial distribution analysis of landslides using FR method

Factor	Class	% class area	% landslide	FR	NFR
Distance to roads (m)	0–100	25.802	85.106	3.298	0.724
	100–200	16.806	10.638	0.633	0.139
	200–300	12.734	0	0	0
	300–400	9.935	0	0	0
	400–500	7.93	2.128	0.268	0.059
	500–600	5.966	2.128	0.357	0.078
	600–700	4.554	0	0	0
	700–800	3.193	0	0	0
	800–900	2.42	0	0	0
	900–1000	2.107	0	0	0
>1000	8.553	0	0	0	
Distance to faults (m)	0–100	6.424	8.511	1.325	0.09
	100–200	5.958	12.766	2.143	0.145
	200–300	5.72	2.128	0.372	0.025
	300–400	5.528	6.383	1.155	0.078
	400–500	5.293	6.383	1.206	0.082
	500–600	5.115	4.255	0.832	0.056
	600–700	4.991	2.128	0.426	0.029
	700–800	4.847	17.021	3.512	0.238
	800–900	4.615	10.638	2.305	0.156
	900–1000	4.586	4.255	0.928	0.063
>1000	46.922	25.532	0.544	0.037	
Distance to drainage (m)	0–100	40.8	44.681	1.095	0.309
	100–200	30.05	40.426	1.345	0.38
	200–300	18.829	10.638	0.565	0.16
	300–400	7.954	4.255	0.535	0.151
	400–500	1.814	0	0	0
	500–600	0.495	0	0	0
	600–703	0.058	0	0	0
Distance to geological boundaries (m)	0–100	15.807	17.021	1.077	0.104
	100–200	13.883	4.255	0.306	0.03
	200–300	12.169	10.638	0.874	0.084
	300–400	11.244	12.766	1.135	0.109
	400–500	10.079	12.766	1.267	0.122
	500–600	8.266	6.383	0.772	0.074
	600–700	6.235	4.255	0.682	0.066
	700–800	4.384	4.255	0.971	0.094
	800–900	3.699	4.255	1.15	0.111
	900–1000	3.284	0	0	0
	>1000	10.95	23.404	2.137	0.206

the road system has altered the natural slope, resulting in an imbalance that increases the probability of landslides. Since precipitation is the main trigger of landslides in the study area, landslides frequently occur along drainage systems, where soil and rock are highly saturated because of rainwater infiltration. However, the distribution of landslides within the classes of the remaining two factors is relatively equal.

Figures 4, 5, and 6 represent the outcomes of the fractal-based analysis. The $\ln(S)$ - $\ln(r)$ plots were linearly fitted with a correlation coefficient of $R^2 > 0.995$, as indicated in the figures. Similar to the results of the previous study (Zuo

and Carranza 2017), these graphs demonstrate a non-linear spatial relationship between the number of landslides or landslide density and distance to conditioning factors. By utilizing a data set based on the number of landslides (case study 1), fractal analyses have shown that the distance to drainage is the most influencing factor in the formation of landslides ($D = 2.0088$). However, using datasets based on relative landslide density (case study 2) and landslide density (case study 3), the analysis results indicated that the distance to geological boundaries has the most significant role in the landslide process. The remaining factors (distance to faults,

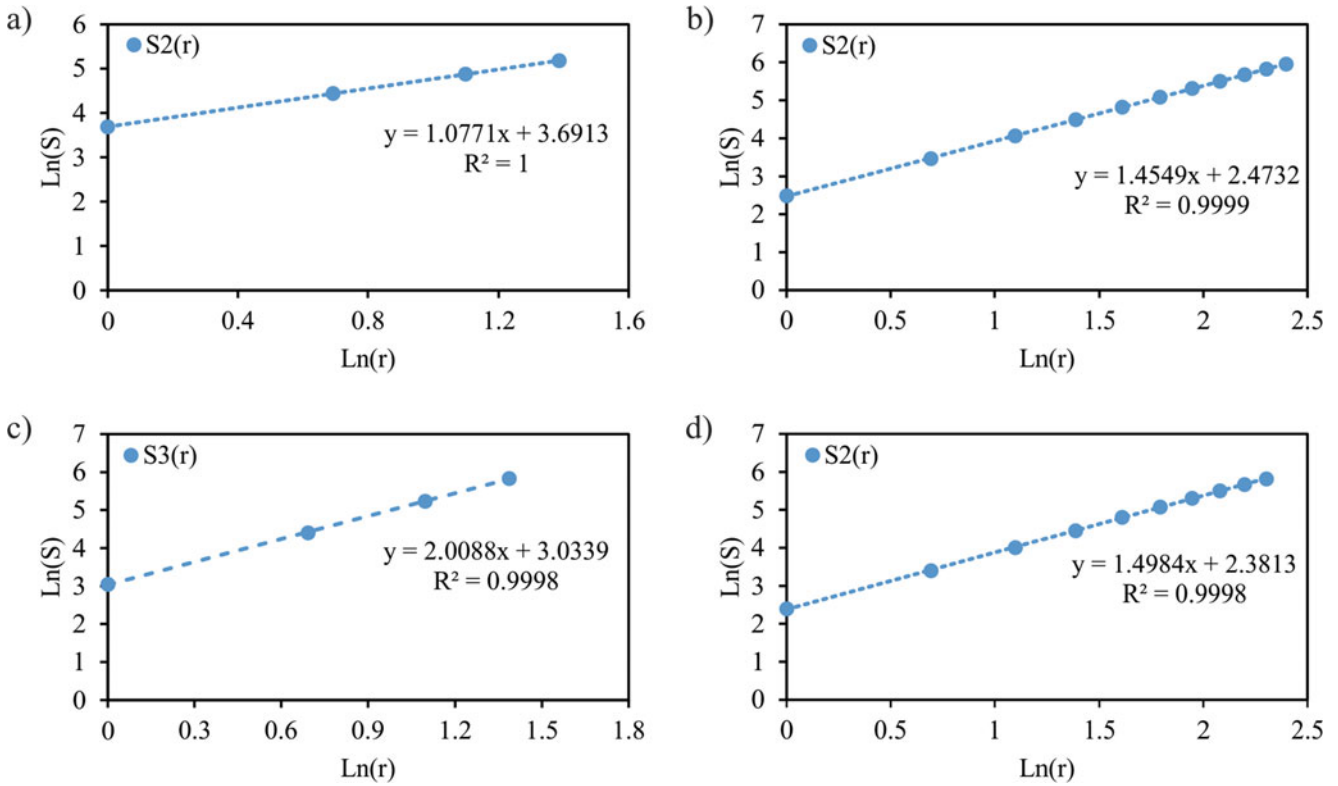


Fig. 4 Fractal analysis using the number of landslides. Graphs of factors: distance to roads (a), distances to faults (b), distance to drainage (c), and distance to geological boundaries (d)

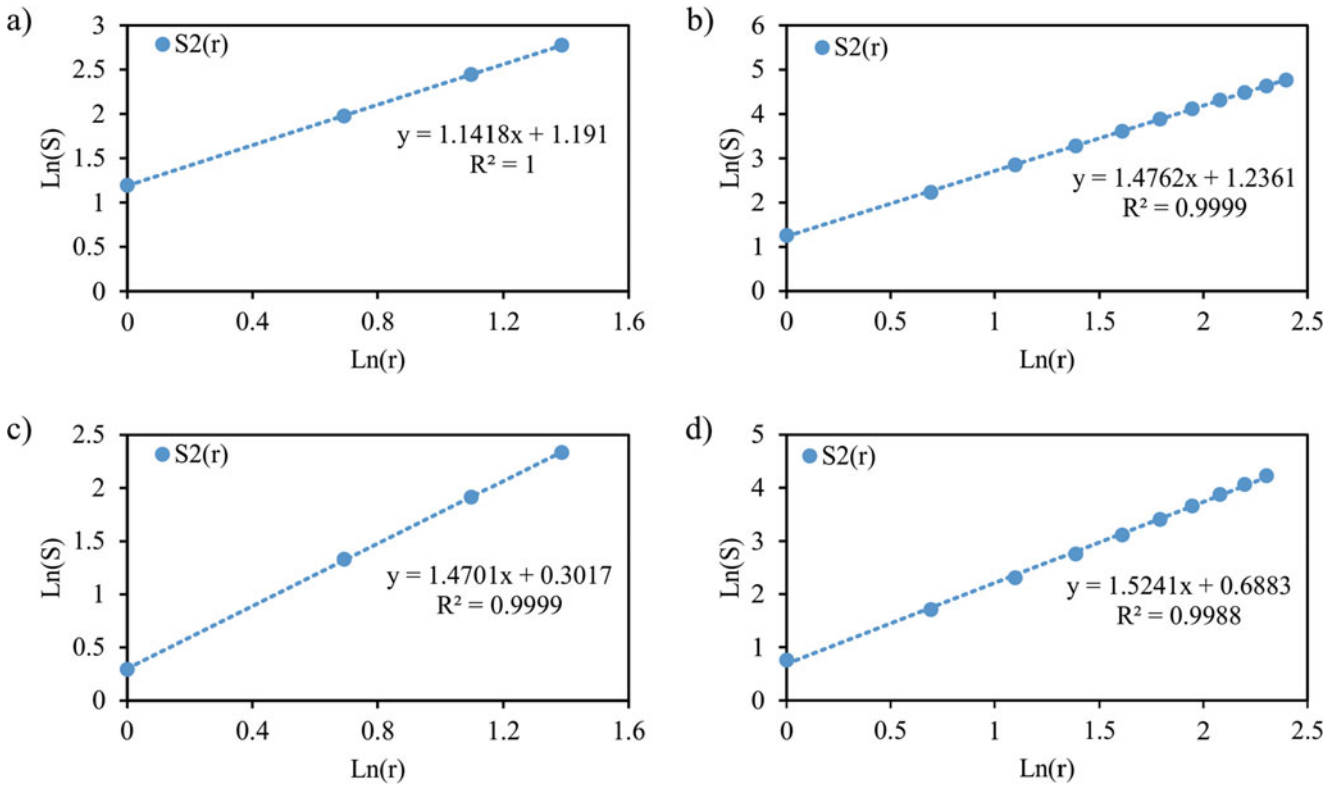


Fig. 5 Fractal analysis using relative landslide density. Graphs of factors: distance to roads (a), distances to faults (b), distance to drainage (c), and distance to geological boundaries (d)

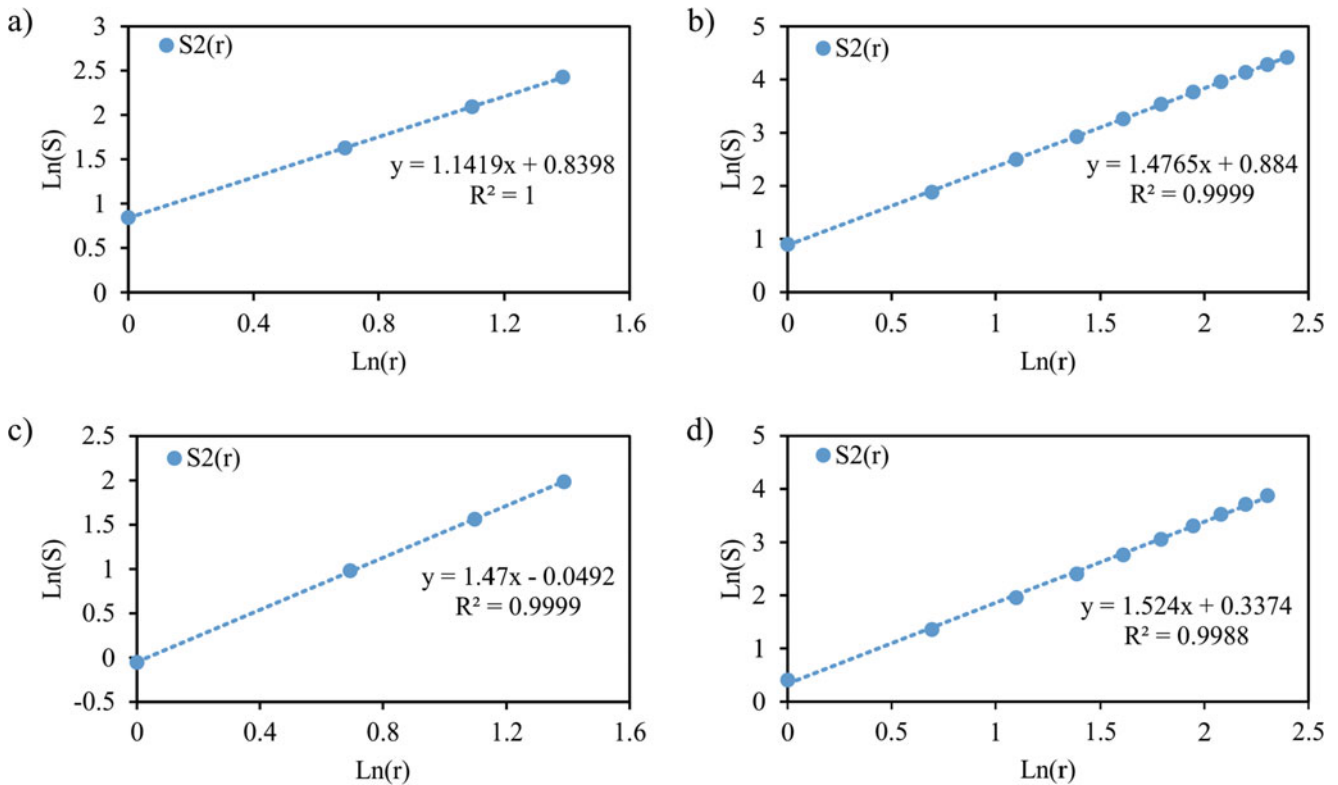


Fig. 6 Fractal analysis using landslide density. Graphs of factors: distance to roads (a), distances to faults (b), distance to drainage (c), and distance to geological boundaries (d)

Table 2 Weights of the factors calculated from fractal analysis

Factor	Case study 1		Case study 2		Case study 3	
	D_i	W_i	D_i	W_i	D_i	W_i
Distance to roads	1.0771	0.178	1.1418	0.203	1.1419	0.203
Distance to faults	1.4549	0.241	1.4762	0.263	1.4765	0.263
Distance to drainage	2.0088	0.333	1.4701	0.262	1.4700	0.262
Distance to geological boundaries	1.4984	0.248	1.5241	0.272	1.5240	0.272

distance to drainage, and distance to roads) have a less significant effect on the landslide process. Based on the formula (3), the D values are then used to calculate the weighted values of the factors (W). The results of the calculations are presented in Table 2.

Using a hybrid fractal-frequency ratio (FFR) model, LSZ maps were produced to compare various data sets for spatial relationship analysis. This model utilizes the results of calculating factor class weights using the frequency ratio method and factor weights using the fractal method. The FFR1 model employs the analysis results of case study 1, while the FFR2 model reflects case studies 2 and 3. A receiver operating characteristic (ROC) analysis was conducted to assess the performance of these models.

3.3 Model Validation

In this study, the well-known ROC method was employed to assess the accuracy of the prediction maps produced by the two models. A ROC curve is a curve in the unit square formed by plotting sensitivity (or True Positive Rate—TPR) versus specificity ($1 - \text{FPR}$, FPR —False Positive Rate) at different thresholds (Yu et al. 2021). It is widely accepted that a higher and more leftward-positioned ROC curve in the ROC space indicates better prediction performance (Metz 1978). Based on the landslide inventory map, which included 47 landslides, ROC analyses were conducted to determine the AUC-ROC (area under the ROC curve) value.

3.4 Results of Landslide Susceptibility Using Fractal-Frequency Method (FFR)

The LSI values for the study area were calculated using Eq. (6) to produce landslide susceptibility index maps. The LSI values range from 0.006 to 0.363 (FFR1) and 0.006 to 0.365 (FFR2). Based on the landslide susceptibility index (LSI) maps, we prepared the landslide susceptibility zonation (LSZ) maps in ArcGIS using the Jenks natural breaks classification method. The study area was divided into five landslide susceptibility zones: very low, low, moderate, high, and very high (Figs. 7 and 8). The LSZ maps produced by the two models have similarities when determining the spatial distribution of susceptibility zones. Most high and very high susceptibility zones were identified at low to moderate elevations and are dominated by road and drainage networks. It has also been shown that the fault system and geological boundaries in the study area affect the spatial distribution of these zones.

The proportion of each landslide susceptibility zone predicted by the two models is shown in Fig. 9. As seen in Fig. 9, all susceptibility zones to landslides were assessed similarly by all two models. The very high susceptibility zone predicted by the two models is 24.34 (FFR1) and 25.52% (FFR2). In addition, the very low landslide susceptibility zones assessed by these models are 17.91% and 17.66%, respectively.

By using 47 past landslides in the study area, ROC curves depicting the performance of two models were constructed (Fig. 10). In Fig. 10, the AUC values and ROC curves indicated very good model performance in predicting the spatial distribution of landslides (AUC > 80%) (Swets 1988). All models revealed a relationship between landslide conditioning factors and the distribution of historical landslides in the study area, as shown by an analysis of the

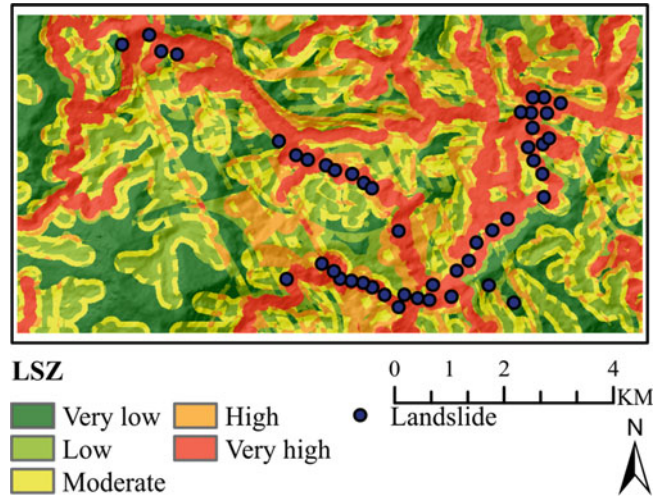


Fig. 8 LSZ map using FFR2 model

success rate curves. Generally, the area under the curve (AUC) values of the success rate curves for the FFR1 and FFR2 models are almost identical. Simultaneously, the analysis outcomes revealed that the FFR2 model performed slightly better than the FFR1 model, indicating strong model performance and prediction accuracy.

According to the study results, all three raw data sets may be utilized to analyze the relationship between landslides and conditioning factors. However, the model using landslide density-based data provides improved prediction performance. This result may be explained by the fact that the landslide density provides a stronger spatial relationship between the distribution of landslides and the area of the factor subclasses. This difference may be defined more clearly if the study is conducted in a region with a significant number of landslides, along with conditioning factors selected depending on data availability, features of landslides, and previous studies in the study area.

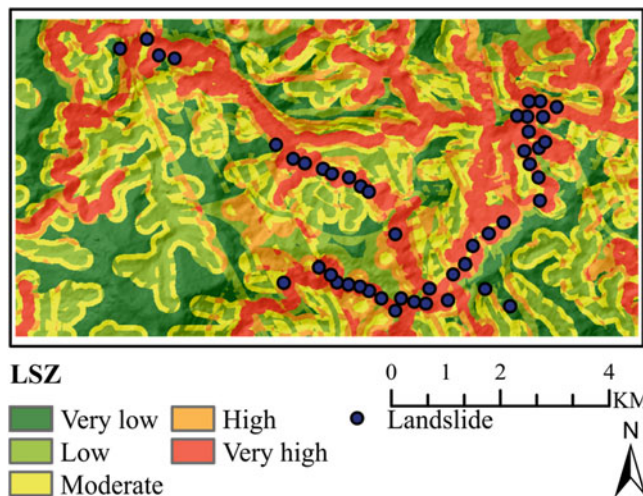


Fig. 7 LSZ map using FFR1 model

4 Conclusions

In landslide hazard and susceptibility studies, the efficacy of assessing the relationship between past landslides and selected factors is crucial to the accuracy of the produced maps. Therefore, this study was conducted to determine the effect of several factors on the distribution of landslides in Tinh Tuc town, Cao Bang province, Vietnam. Three raw data sets were generated using the number of landslides and landslide density. By utilizing the frequency ratio method and the fractal method, the role of subclasses and factors, as expressed by NFR and W values, was evaluated. Afterward, two landslide susceptibility maps were produced based on the selected data sets. The similarity of the susceptibility zone predicted by the two models and the outcomes of the ROC

Fig. 9 Distribution of susceptibility zones for each model

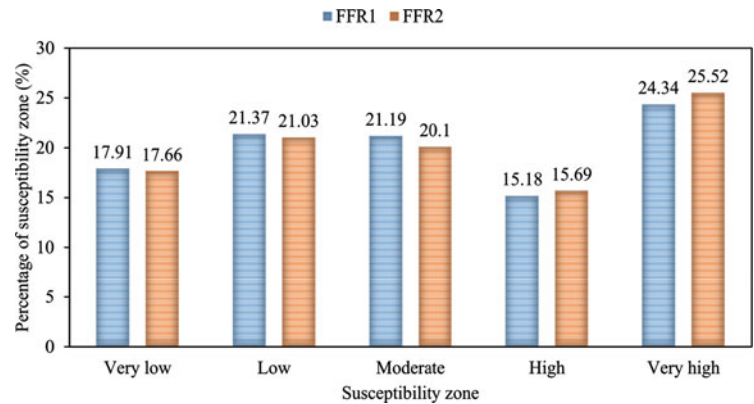
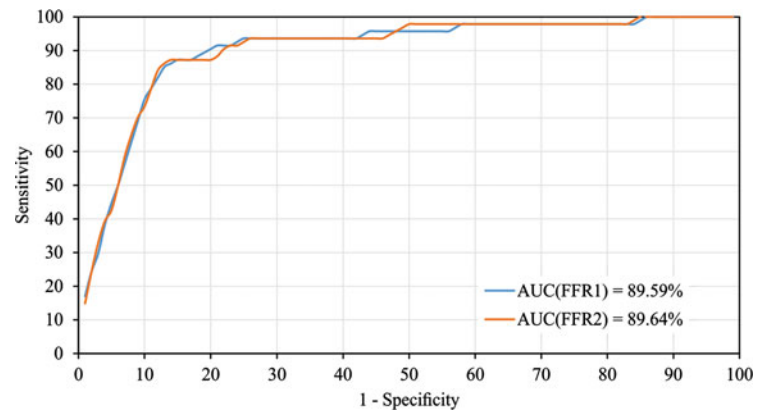


Fig. 10 ROC curves with AUC values of two models



analysis revealed that the data sets are suitable for producing highly accurate landslide susceptibility maps. It is suggested to apply the fractal method in landslide susceptibility studies because it is possible to quantify the influence of conditioning factors, thereby improving the accuracy of landslide prediction.

Acknowledgments We would like to express our gratitude to the Institute of Geological Sciences, Vietnam Academy of Science and Technology, and the national science and technology project under grant number ĐTDL.CN-81/21 for supplying analysis data.

References

- Bien TX, Truyen PT, Phong TV, Nguyen DD, Amiri M, Costache R, Duc DM, Le HV, Nguyen HBT, Prakash I, Pham BT (2022) Landslide susceptibility mapping at sin Ho, Lai Chau province, Vietnam using ensemble models based on fuzzy unordered rules induction algorithm. *Geocarto Int* 1–22. <https://doi.org/10.1080/10106049.2022.2136253>
- Cello G, Malamud BD (2006) Fractal analysis for natural hazards. Geological Society, London. ISBN: 9781862392014. 261 p. <https://doi.org/10.1144/GSL.SP.2006.261>
- Do NH, Goto S, Abe S, Nguyen KT, Miyagi T, Hayashi K, Watanabe O (2022) Torrent rainfall-induced large-scale karst limestone slope collapse at Khanh waterfall, Hoa Binh Province, Vietnam. *Geoenviron Disasters* 9(1). <https://doi.org/10.1186/s40677-022-00206-5>
- Elejalde-Cadena NR, Moreno A (2021) Fractal analysis of the distribution and morphology of pores in dinosaur eggshells collected in Mexico: implications to understand the biomineralization of calcium carbonate. *ACS Omega* 6(11):7887–7895. <https://doi.org/10.1021/acsomega.1c00478>
- Hu Q, Zhou Y, Wang SX, Wang FT, Wang HJ (2020) Fractal-based spatial distribution analysis of geological hazards and measurement of spatial association with hazard-related predisposing factors. *Int Arch Photogramm Remote Sens Spatial Inf Sci XLII-3/W10125–131*. <https://doi.org/10.5194/isprs-archives-XLII-3-W10125-2020>
- Hung LQ, Van NTH, Son PV, Ninh NH, Tam N, Huyen NT (2017) Landslide inventory mapping in the fourteen Northern Provinces of Vietnam: achievements and difficulties. In: Sassa K, Mikoš M, Yin Y (eds) *Advancing culture of living with landslides*. Springer International Publishing, Cham. ISBN: 978-3-319-59,469-9, pp 501–510. https://doi.org/10.1007/978-3-319-59,469-9_44
- Kien NT, Tran TV, Lien VTH, Linh PLH, Thanh NQ (2021) Landslide susceptibility mapping based on the combination of bivariate statistics and modified analytic hierarchy process methods: a case study of Tinh Tuc Town, Nguyen Binh District, Cao Bang Province, Vietnam. *J Disaster Res* 16(4):521–528. <https://doi.org/10.20965/jdr.2021.p0521>
- Lan Huong TT, Van Anh DT, Dat TT, Truong DD, Tam DD (2022) Disaster risk management system in Vietnam: progress and challenges. *Heliyon* 8(10). <https://doi.org/10.1016/j.heliyon.2022.e10701>
- Liao M, Wen H, Yang L (2022) Identifying the essential conditioning factors of landslide susceptibility models under different grid resolutions using hybrid machine learning: a case of Wushan and Wuxi counties, China. *CATENA* 217. <https://doi.org/10.1016/j.catena.2022.106428>

- Mandelbrot B (1967) How long is the coast of Britain? Statistical self-similarity and fractional dimension. *Science* 156(3775):636–638
- Metz CE (1978) Basic principles of ROC analysis. *Semin Nuclear Med* 8(4):283–298. [https://doi.org/10.1016/S0001-2998\(78\)80014-2](https://doi.org/10.1016/S0001-2998(78)80014-2)
- Paun M-A, Paun V-A, Paun V-P (2022) Fractal analysis and time series application in ZY-4 SEM micro fractographies evaluation. *Fractal Fractional* 6(8). <https://doi.org/10.3390/fractalfract6080458>
- Pham TT, Nong ND, Sathyan AR, Garschagen M (2020) Vulnerability assessment of households to flash floods and landslides in the poor upland regions of Vietnam. *Climate Risk Manage* 28. <https://doi.org/10.1016/j.crm.2020.100215>
- Santuz A, Akay T (2020) Fractal analysis of muscle activity patterns during locomotion: pitfalls and how to avoid them. *J Neurophysiol* 124(4):1083–1091. <https://doi.org/10.1152/jn.00360.2020>
- Swets JA (1988) Measuring the accuracy of diagnostic systems. *Science* 240(4857):1285–1293. <https://doi.org/10.1126/science.3287615>
- Tanabe N, Sato S, Suki B, Hirai T (2020) Fractal analysis of lung structure in chronic obstructive pulmonary disease. 11. <https://doi.org/10.3389/fphys.2020.603197>
- Tien Bui D, Tuan TA, Hoang N-D, Thanh NQ, Nguyen DB, Van Liem N, Pradhan B (2017) Spatial prediction of rainfall-induced landslides for the Lao Cai area (Vietnam) using a hybrid intelligent approach of least squares support vector machines inference model and artificial bee colony optimization. *Landslides* 14(2):447–458. <https://doi.org/10.1007/s10346-016-0711-9>
- VIGMR (2017) Report on landslide hazard zonation in Cao Bang province (in Vie). Ministry of Natural Resources and Environment, Hanoi
- Wang Y, Sun D, Wen H, Zhang H, Zhang F (2020) Comparison of random forest model and frequency ratio model for landslide susceptibility mapping (LSM) in Yunyang County (Chongqing, China). *Int J Environ Res Public Health* 17(12). <https://doi.org/10.3390/ijerph17124206>
- Yu X, Zhang K, Song Y, Jiang W, Zhou J (2021) Study on landslide susceptibility mapping based on rock-soil characteristic factors. *Sci Rep* 11(1). <https://doi.org/10.1038/s41598-021-94,936-5>
- Zuo R, Carranza EJM (2017) A fractal measure of spatial association between landslides and conditioning factors. *J Earth Sci* 28(4): 588–594. <https://doi.org/10.1007/s12583-017-0772-2>

Open Access This chapter is licensed under the terms of the Creative Commons Attribution 4.0 International License (<http://creativecommons.org/licenses/by/4.0/>), which permits use, sharing, adaptation, distribution and reproduction in any medium or format, as long as you give appropriate credit to the original author(s) and the source, provide a link to the Creative Commons license and indicate if changes were made.

The images or other third party material in this chapter are included in the chapter's Creative Commons license, unless indicated otherwise in a credit line to the material. If material is not included in the chapter's Creative Commons license and your intended use is not permitted by statutory regulation or exceeds the permitted use, you will need to obtain permission directly from the copyright holder.

